

# Analysis of Polymer Flow in Nanoimprint Lithography Based on Finite Element Method

Hongwen Sun<sup>1,2,3,\*</sup>, Ping Wan<sup>1,4</sup>, and Jianjun Ni<sup>1,2,3</sup>

<sup>1</sup>College of Internet of Things, Hohai University, 200 Jinling Road North, Changzhou, 213022, China

<sup>2</sup>Jiangsu Key Laboratory of Power Transmission and Distribution Equipment Technology, 200 Jinling Road North, Changzhou, 213022, China

<sup>3</sup>Changzhou Key Laboratory of Sensor Networks and Environmental Sensing, 200 Jinling Road North, Changzhou, 213022, China

<sup>4</sup>Changzhou Liu Guojun Vocational Technology College, 200 Jinling Road North, Changzhou, 213022, China

Thermal nanoimprint lithography (NIL) has the advantage of high resolution and low cost, however it requires a significant amount of processing time. Finite element analysis (FEA) simulation can save research time and cost and help to understand the behavior of the polymer flow. ANSYS was employed to set up a nonlinear hyperelastic FEA model. The model was applied to analyze the resist flow during the NIL process. When the width of the stamp cavity increases or the resist thickness increases, the external pressure needed for resist flow decreases and the resist flows more easily. While the cavity depth becomes deeper, the resist needs bigger external pressure in order to fill in the cavity fully.

**Keywords:** Nanoimprint Lithography (NIL), Finite Element Analysis (FEA), ANSYS, Resist Flow, Simulation, Polymer Deformation.

## 1. INTRODUCTION

In the nano era, nanostructures are widely studied<sup>1-3</sup> and researchers have strong interest in fabricating smaller nanostructures. With the continuing demand of shrinking feature size in the semiconductor field,<sup>4</sup> the traditional lithography technology is facing severe challenges. Nanoimprint lithography (NIL)<sup>5-7</sup> avoid the problems such as light diffraction in optical lithography. The resist is formed by physics pressing. The minimum feature size of this technology can be achieved at 5 nm.<sup>8</sup>

In nanoimprint process, it is crucial to know how the polymer fills template cavities. Simulation study of nanoimprint process can save time and money. The research methods on this field include viscoelastic Newton fluid model, molecular dynamics model and finite element model.

Viscoelastic fluid model<sup>9</sup> employs Newton commercial computational fluid dynamics software CFD-ACE, applies a finite volume theory to trace polymeric boundary deformation based on the Eulerian grid and volume of fluid (VOF) theory. This model has a fatal flaw: when the boundary velocity of the fluid is larger, fluid boundary tracking accuracy will be greatly reduced. In NIL process,

the fluid boundary velocity is larger. If VOF model is used, the boundary condition is too rough, which will affect the simulation results.

Molecular dynamics<sup>10</sup> is an important computer simulation method to solve interaction issues among multiple degree freedom system based at the atomic level. By solving all atomics' motion equations, it can be employed to simulate detail process related to atomic motion path. Because the sample in NIL has a short relaxation time, the absorbed energy of the sample will increase dramatically. If the energy exceeds the critical value, the simulation will be unsuccessful.

Several groups have simulated NIL process using the finite element method. Kim et al. analyzed the deformation behaviors of polymeric stamps using the slip-link model.<sup>11</sup> Hirai et al. used the commercially available software MARC to study the imprint pressures required for successful imprinting and the filling rate into the mold grooves according to different aspect ratio of the pattern, initial polymer thickness and duty ration of the pattern.<sup>12</sup> A simulation model was developed based on a viscous model to predict the polymer flow behavior during the imprinting.<sup>13</sup> Song and Kim et al. used FEM method to simulate low temperature thermal NIL process using a viscoelastic model.<sup>14,15</sup> Ryu et al. reported their FEM analysis

\*Author to whom correspondence should be addressed.

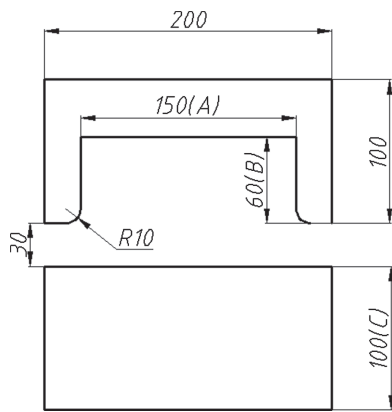


**Fig. 1.** Finite element model of a cell (unit: nm, *A* stands for cavity width, *B* cavity depth, *C* initial resist thickness).

**Table I.** Material parameters.

Material	Density (kg/m <sup>3</sup> )	<i>E</i> (GPa)	$\nu$
PMMA	1200	0.9	0.499
Si	2300	190	0.3

of indentation stress induced in mold materials when they come in contact with 1 MPa expanded uniaxial stress.<sup>16</sup> Sun et al. employed DEFORM to analyze different imprint factors such as imprint temperature, pressure and time when imprinting grating structures.<sup>17</sup> However, there are few group researched NIL process using ANSYS simulation. ANSYS can provide richness of functionality across a broad range of disciplines including structural, fluids and thermal, which are the fields related to nanoimprint. The ANSYS capability in multiphysics is flexible, robust and architected in ANSYS Workbench to enable to solve complex coupled physics analyses in a unified environment, which is suitable for the optimization of complex NIL processes. One nonlinear hyperelastic NIL model was established in this paper to carry on the simulation analysis by using ANSYS. Nonlinear hyperelastic model has the advantage of matching the real NIL process. Through the research on parameter interactions among mold displacement and stress, cavity width and height and resist

thickness, the influence of each factor to resist filling was investigated in detail.

## 2. SIMULATION METHOD

ANSYS was used to simulate the resist flow in NIL. Figure 1 is the size chart for one unit of the finite element model. The stamp protrusion width is the same with stamp cavity width. The material for template is Si and for resist is PMMA. The thickness and width of the template, the groove depth and width in template, and the initial thickness of polymer are respectively defined in Figure 1. The material properties are shown in Table I.

Due to nonlinearity of this model, nonlinear contact method was taken to simulate the filling process. The assumption was made that there was no sliding displacement between the mold and the polymer. The contact mode was chosen as Rough. In the choice of contact surface and the target plane, generally the surface not easily deformed was chosen as the target plane, and the surface easy deformed as the contact surface. Therefore, in this model the bottom surface of the mold was chosen as the target plane and the top surface of the polymer as the contact surface. In order to speed up the calculation, coarse grid was applied to the mold with little deformation and fine grid to the polymer with larger deformation. The imprint temperature was set up at 150 °C and low viscosity of 10 cP was set for PMMA during 150 °C for all the simulations. The whole deformation was divided into three stages: initial contact, polymer elevated, and final contact, as shown in Figure 2.

## 3. RESULTS AND DISCUSSION

### 3.1. Overall Deformation

In the process of nanoimprint, with the pressing force by the mold, the polymer generate large deformation and fill the cavities of the mold. The polymer contacted with the elevated part of the mold is firstly pressed, and this part of polymer is extruded to the central cavity of the mold. The polymer gradually fill all the cavities of the mold when imprint time increases. The time of the fill process was set as 1 minute for all pressure condition. From

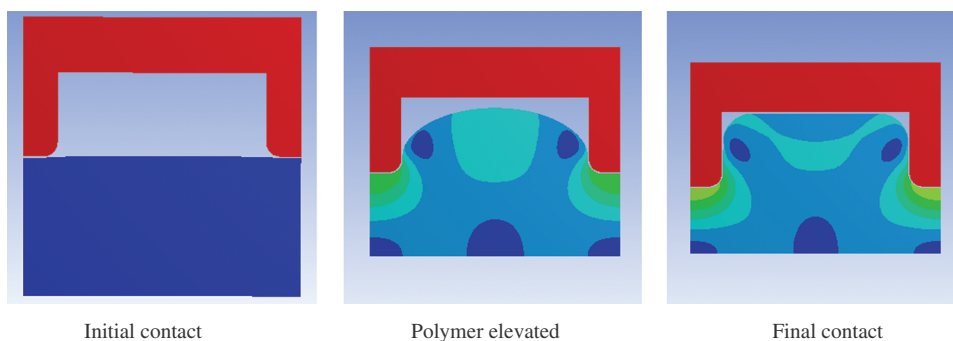


**Fig. 2.** Three stages of the whole deformation process.

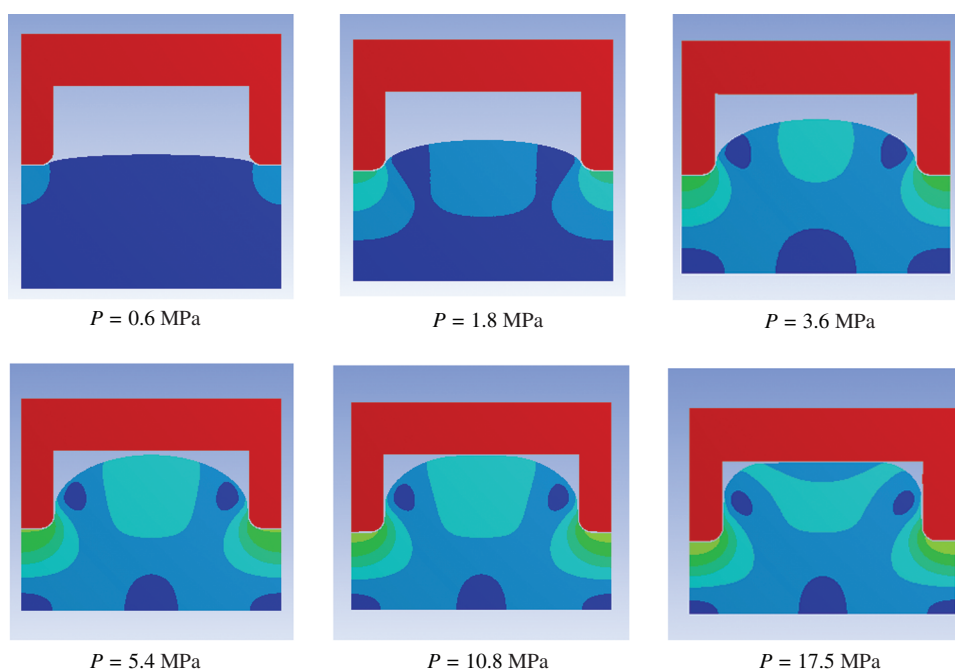


Fig. 3. Resist deformation with different imprint pressure.

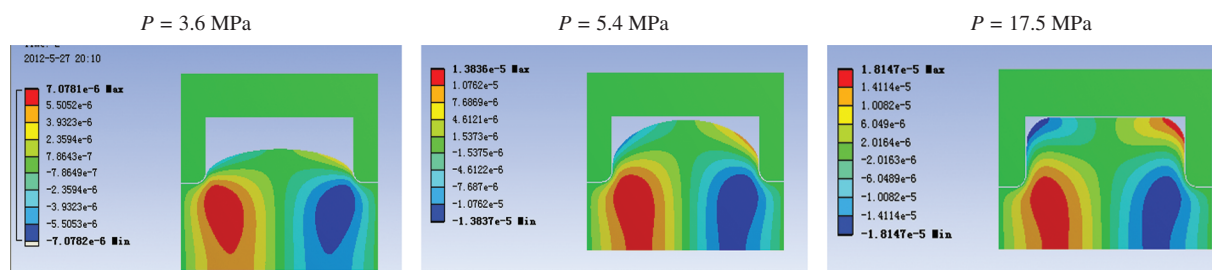


Fig. 4. Resist elastic deformation in X direction with different imprint pressure.

Figure 3, it can be shown that the ends part of the polymer have larger deformation than the central part with different imprint pressure.

### 3.2. X Direction and Y Direction Deformation

When the resist is pressed by a stamp, the resist will produce the elastic deformation in X direction and Y direction. Figure 4 shows the resist elastic deformation in X direction with different imprint pressure. With the stress

applied by the elevated parts of the stamp, the lower part of the resist generates inward convergence, and the top part of the resist is dissipated outward. The right part of the resist flows in a clockwise direction and the left part in a anticlockwise direction. By this way, the resist fully fills the whole cavity of the stamp.

Figure 5 gives the resist elastic deformation in Y direction with different imprint pressure. Due to the compression force by the stamp, the central part of the resist is

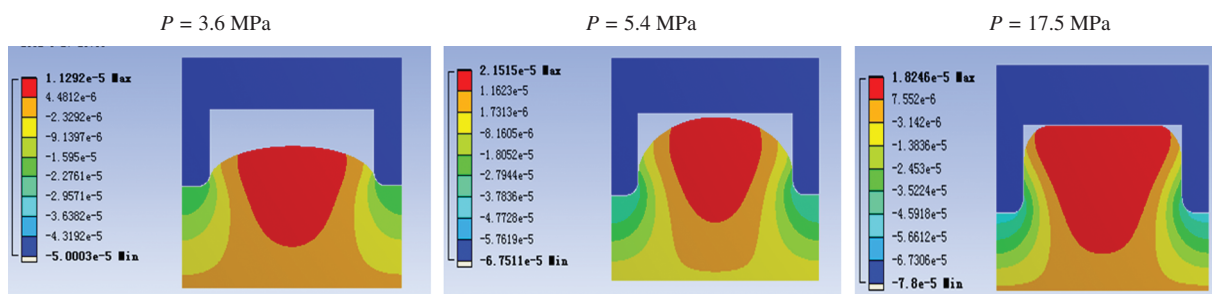


Fig. 5. Resist elastic deformation in Y direction with different imprint pressure.

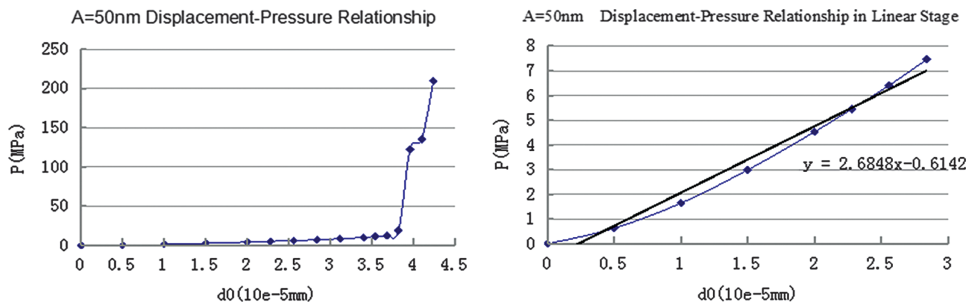


Fig. 6. Relationship between stamp displacement and pressure when  $A = 50$  nm.

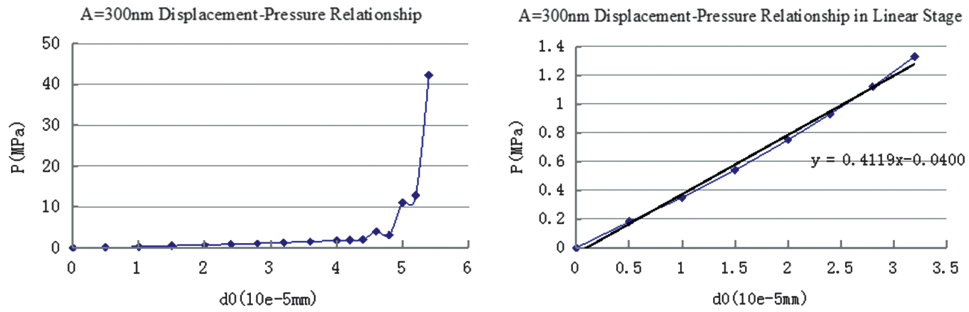


Fig. 7. Relationship between stamp displacement and pressure when  $A = 300$  nm.

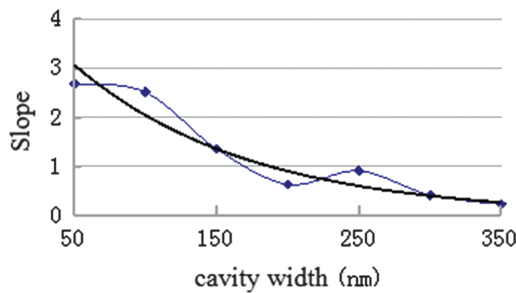


Fig. 8. Slope of the curve for different cavity width.

raised, and the left and right part of the resist flows downward. Similar to the deformation in the  $X$  direction, the right part of the resist flows in a clockwise direction and the left part in a anticlockwise direction.

### 3.3. Influence of Cavity Width on Resist Flow

As shown in Figures 6 and 7, along with the cavity width increases, space for resist flow also increases, and resist

inner stress decreases. The resist flow ability in the cavity becomes strong, and the pressure needed to apply to stamp decreases. Linear fitting for the data of linear stage was carried out. By this way, the slope of the curve for different cavity width can be achieved and the slope can be expressed as  $\partial d0/\partial P$ . It stands for the unit stress needed to generate the unit stamp displacement. Due to the initial displacement length and pressure are both zero, the required external pressure and resist flow ability for different cavity width can be known through the slope of the curve. The smaller the slope, the smaller external pressure needed for an unit displacement, which means the smaller of needed external pressure for resist deformation and more easily the resist flows. Figure 8 shows the slope of the curve for different cavity width.

### 3.4. Influence of Cavity Depth on Resist Flow

From Figures 9 and 10, it can be seen that with the increase of the cavity depth, there is more room for the

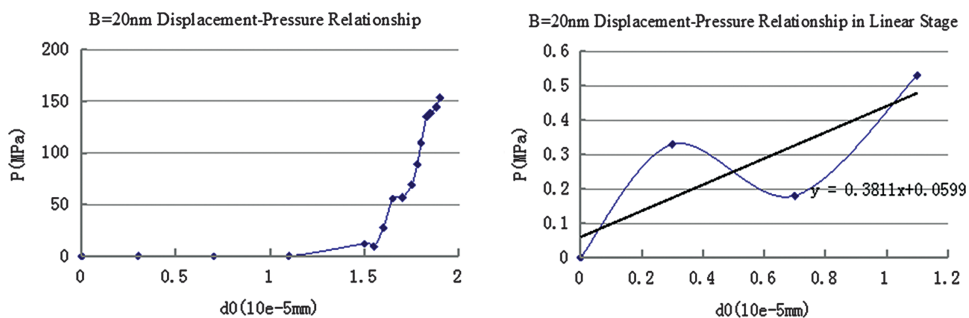


Fig. 9. Relationship between stamp displacement and pressure when  $B = 20$  nm.

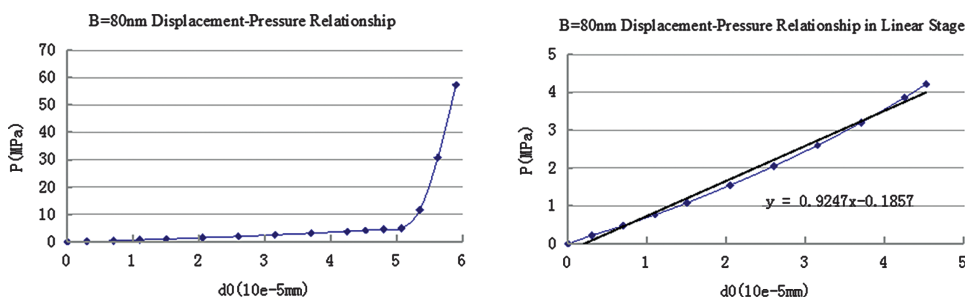


Fig. 10. Relationship between stamp displacement and pressure when  $B = 80$  nm.

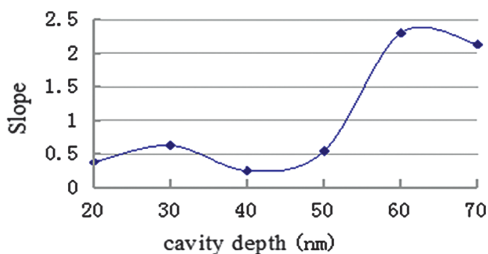


Fig. 11. Slope of the curve for different cavity depth.

resist to fill in. In order to let the resist fully fill in the cavity, it needs bigger external pressure. Through the study the mutual relationship between displacement and external pressure, one can know directly the resist flow with different cavity depth. However, due to the change of cavity depth, the inner area of the cavity also changes with it as well as the maximum displacement for the stamp. Linear fitting for the data of linear stage was carried out to find out

the slope of curves with different cavity depth. The slope can be expressed by  $\partial d0 / \partial P$ . The analysis is similar to the one for cavity width. The result is shown in Figure 11.

**3.5. Influence of Resist Thickness on Resist Flow**

From Figures 12 and 13, it can be shown that when resist thickness increases, the resist amount used to fill in the stamp cavity also increases. This induces the needed force for deformation decreases, which means external pressure decreases. By research on the mutual relationship between displacement and external pressure, one can know easily the resist flow characteristic in the condition of different resist thickness. Similar to the analysis method above, linear fitting was carried out based on data of linear stage. The slope of the curve was achieved for different resist thickness, as shown in Figure 14.

The paper deals with ANSYS finite element analysis on nanoimprinted nanostructures. It provides a fast,

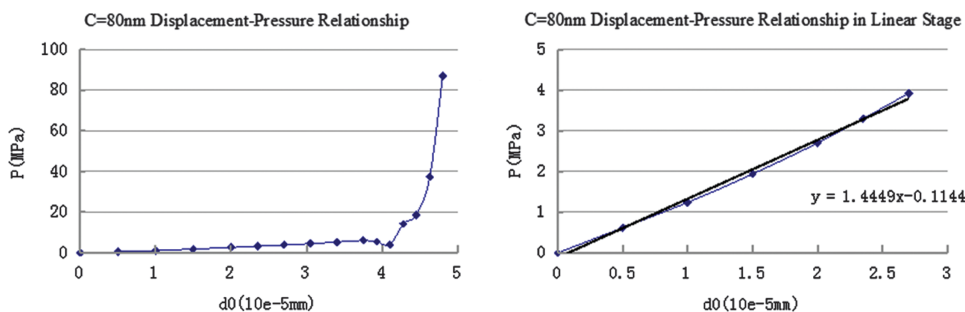


Fig. 12. Relationship between stamp displacement and pressure when  $C = 80$  nm.

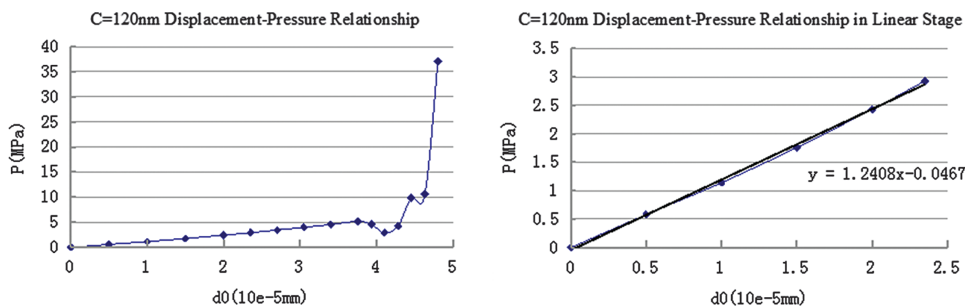


Fig. 13. Relationship between stamp displacement and pressure when  $C = 120$  nm.

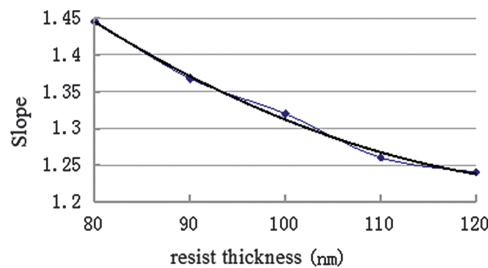


Fig. 14. Slope of the curve for different resist thickness.

straightford and 3D visiable simulation, compared to quantum theory analysis, which is still to be an open question.<sup>18, 19</sup>

#### 4. CONCLUSIONS

Nonlinear hyperelastic finite element model was established based on ANSYS to analyze nanoimprint process. With different stamp cavity width, depth and resist thickness, the relationship between stamp displacement and external pressure was researched respectively, in order to know the effect of different factors on resist flow. When the stamp cavity width increases, the external pressure needed for resist flow decreases and resist flows more easily. With cavity depth deeper, the resist is harder to flow and needs bigger external pressure. While the resist thickness increases, it is more easily to fill in the cavity with less external pressure. FEM analysis on NIL can help researchers to better understand the polymer flow behavior during the imprinting process.

**Acknowledgments:** This research was supported by the National Science Foundation of China (NSFC: 61203365) and by the Natural Science Foundation of Jiangsu Province, China (NSF Jiangsu: BK2012149).

#### References

1. P. K. Bose, N. Paitya, S. Bhattacharya, D. De, S. Saha, K. M. Chatterjee, S. Pahari, and K. P. Ghatak, *Quantum Matter* 1, 89 (2012)
2. B. Tüzün and C. Erkoç, *Quantum Matter* 1, 136 (2012)
3. T. Ono, Y. Fujimoto, and S. Tsukamoto, *Quantum Matter* 1, 4 (2012)
4. Z. Johari, F. Khairiah, A. Hamid, M. T. Ahmadi, F. K. C. Harun, and R. Ismail, *J. Comput. Theor. Nanosci.* 10, 1305 (2013)
5. S. Y. Chou, P. R. Krauss, and P. J. Renstrom, *Science* 272, 85 (1996).
6. L. J. Guo, *Adv. Mater.* 19, 495 (2007).
7. B. Radha, S. H. Lim, M. S. M. Saifullah and G. U. Kulkarni, *Scientific Reports* 3, 1 (2013).
8. M. D. Austrin, H. X. Ge, and W. Wu, *Appl. Phys. Lett.* 84, 5299 (2004).
9. H. D. Rowland, A. C. Sun, P. R. Schunk, and W. P. King, *J. Micromech. Microeng.* 15, 2414 (2005).
10. Y. K. Hong, H. J. Hwang, and K.-S. Kim, *J. Comput. Theor. Nanosci.* 10, 1310 (2013)
11. J. H. Kim, J. Y. Kim, and B. I. Choi, *IEEE-Nano* 2, 263 (2003).
12. Y. Hirai, T. Konish, T. Yoshikawa, and S. Yoshida, *J. Vac. Sci. Technol., B* 22, 3288 (2004).
13. W.-B. Young, *Microelectron. Eng.* 77, 405 (2005).
14. J. H. Song, H. Huh, S. H. Kim, and H. T. Hahn, *Mater. Sci. Forum* 505–507, 85 (2006).
15. N. W. Kim, K. W. Kim, and H.-C. Sin, *Microelectron. Eng.* 85, 1858 (2008).
16. R.-H. Ryu, S.-H. Lim, J. I. Jeong, D. Shin, S. Jang, H. J. Yim, and K. S. Lee, *J. Mech. Sci. Technol.* 23, 1031 (2009).
17. H. W. Sun, G. G. Liu, and S. M. Lin, *Computer Application and System Modeling (ICCASM)* V12, 293 (2010).
18. A. Khrennikov, *Rev. Theor. Sci.* 1, 34 (2013).
19. A. Herman, *Rev. Theor. Sci.* 1, 3 (2013).

Received: 14 June 2013. Accepted: 12 July 2013.